

Magnetopause reconnection induced by magnetosheath Hall-MHD fluctuations

G. Belmont, and L. Rezeau

Centre d'étude des Environnements Terrestre et Planétaires, Université de Versailles-St Quentin en Yvelines, Vélizy, France

Abstract. Any penetration of solar wind plasma into the magnetosphere would be precluded if the plasma were strictly frozen in the magnetic field. Such transfers cannot therefore be modeled in the frame of ideal MHD: they demand nonideal effects and are likely to involve reconnection at the magnetopause. The strong magnetic fluctuations observed at this boundary have been suggested for a long time to be responsible for these phenomena. The present study revisits two questions: what is the origin of the strong magnetopause fluctuations and by which mechanisms can they allow for reconnection? It is first confirmed that the preexisting magnetosheath fluctuations can be the primary cause of the strong magnetopause fluctuations. The phenomenon invoked in a preceding paper to explain their amplification, known as “Alfvén resonance,” is ruled out and shown to be an artifact of ideal MHD. The amplification at the boundary is instead explained by a nonresonant mode conversion (due to the magnetopause gradient), followed by a trapping of the resulting Alfvén wave in the boundary (due to the magnetic field rotation). The trapped Alfvén wave has strong amplitude and its finite frequency is responsible for a departure from ideal MHD associated with reconnection distributed all over the magnetopause surface. We evidence that reconnected magnetic flux, driven by the incident magnetosheath waves, is able in this way to penetrate the magnetosphere, and we show how a local reconnection rate can be estimated. This result should be the starting point for a new approach of the magnetopause transfer problem since, in this scenario, reconnection occurs without external electrostatic electric field, as in stationary *X* point models, and without any local instability, as in tearing type models.

1. Introduction

Many experimental observations have evidenced the presence of a high level of electromagnetic fluctuations at the magnetopause and they arouse interest because they are likely to play a driving role in the transfers from the solar wind to the magnetosphere (for a recent review, see *Rezeau and Belmont* [2001]). Recent works have suggested that these fluctuations are not generated in the boundary but result from the interaction of the magnetosheath turbulence with the discontinuity that characterizes the magnetopause. This boundary is well known to be mainly a magnetic boundary, standing between the Earth magnetic field and the solar wind magnetic field. In fact, many other parameters change at once, or within a short distance, in particular the density. In a first paper, *Belmont et al.* [1995] investigated the interaction of a wave coming from the magnetosheath with the magnetopause density gradient, and showed that this interaction could indeed explain the intensification of the electromagnetic turbulence that is observed at the magnetopause. A “resonant amplification” phenomenon was evidenced in the boundary, appearing at the point where the incident wave, propagating initially on the fast mode, meets the Alfvén mode frequency. This phenomenon leads to two results that appear in agreement with the data: an intensification of some wave components and a modification of the polarization. This

model was purely MHD, and the results presented in the particular case of cold plasma, with a unidirectional magnetic field.

Later, *De Keyser et al.* [1999] performed a more realistic study, including in the model the temperature of the plasma and the magnetic shear. Both features are known to be very important at the magnetopause, since the β parameter of the plasma is of the order of 1, and the rotation of the magnetic field can be as large as 180° in some cases. Although the problem is somewhat more complicated, the results are not very different and a resonant amplification still takes place at some points in the boundary.

Nevertheless, this approach to the problem is still not completely realistic, because another parameter has to be taken into account to reproduce the experimental situation. As a matter of fact, the spectrum of the fluctuations observed at the magnetopause is broadband and extends from very low frequencies up to frequencies higher than the proton gyrofrequency [*Rezeau et al.*, 1989]. The pure MHD model, which presupposes a frequency negligible with respect to the gyrofrequency, is therefore not generally applicable. Investigating the interaction of the magnetosheath incident wave with the magnetopause, we will show that ion inertia can never be ignored, even at the lowest frequencies and that it drastically changes the results. A completely kinetic description is not mandatory to evidence this effect: we will restrain ourselves to a Hall-MHD model, leaving the modifications due to the finite Larmor radius effects for a further study. These effects can be introduced in the spirit of the paper by *Johnson and Cheng* [1997], where it was done in

Copyright 2001 by the American Geophysical Union.

Paper number 2000JA900151.
0148-0227/01/2000JA900151\$09.00

a very elegant manner but where the ion inertia was neglected.

The paper is organized as follows: first, the model is presented and the corresponding system of equations established. As the resolution of this system is a difficult mathematical problem, a first step will be a prediction of the possible solutions deduced from the knowledge of the behavior of the waves in a homogeneous medium. Then the mathematical solution will be presented and the solution discussed. As will be shown, this solution has a very interesting feature: a strong Alfvén mode is created in the boundary with a wavelength going very small at some point in the layer. This result opens new prospects that will be discussed in the last section. Actually, one of the interests towards the electromagnetic fluctuations that are observed at the magnetopause is that they could drive reconnection, which is the most popular mechanism to explain the transfers through the boundary. Although a fully quantitative description of the phenomenon cannot be given in the present frame of the Hall-MHD model, it will be shown that the small scales created by the conversion in the boundary are indeed able to create microreconnection locally. An estimate of the efficiency of the mechanism will be given.

2. Model and Equations

The magnetopause is supposed to have a slab geometry (Figure 1). The x axis is the boundary normal ($x < 0$ corresponds to the magnetosheath). The density decreases from ρ_1 to ρ_2 with a $\tanh(x/200)$ law, where x is the distance from the middle of the boundary (in kilometers), which means that the layer is ~ 600 km thick [Berchem and Russell, 1982]. The z axis is the direction of the magnetic field in the magnetosphere. When the rotation of the magnetic field is taken into account, it rotates in the (y, z) plane, with no variation of its modulus: the variations of the magnetic field components are supposed to be hyperbolic, proportional to $1/\cosh(x/200)$ for B_y and $\tanh(x/200)$ for B_z . It means that, for this first step, we consider a total 180° rotation through the

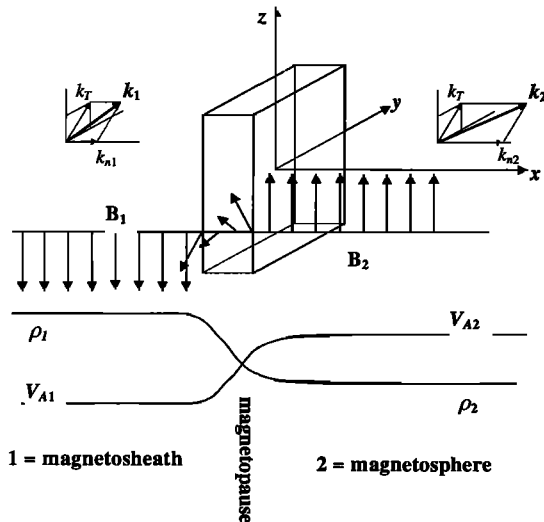


Figure 1. Equilibrium configuration of the model. The variations of the density and the Alfvén velocity are superimposed to the geometrical sketch. The variation of the magnetic field direction is also sketched (for the case with a rotation).

magnetopause. In the future, the role of smaller rotations will have to be investigated. As, for the sake of simplicity, the modulus of the magnetic field is here assumed constant, the pressure also remains constant through the boundary as well as the β parameter; on the contrary, the temperature of the plasma increases to compensate the decrease of the density.

The incident wave is coming from the magnetosheath (that is from the left on Figure 1). It is supposed to be a plane monochromatic wave propagating on the fast mode, with an incident wave vector \mathbf{k}_i . As the problem is invariant in the y and z directions, the component k_T of the wave vector tangential to the discontinuity is constant through the crossing. Therefore the transmitted \mathbf{k}_t wave vector has the same k_T projection and a modified normal component.

To explore the interaction of an incident wave with the magnetopause as it has just been described, we need to use a linearized system of equations that is extended with respect to the preceding ideal MHD model. To take into account the finite frequency effects, the ion inertia terms have to be included in the system [Belmont and Rezeau, 1987] and they appear in the Ohm's law, which writes:

$$\mathbf{E} = -\mathbf{v} \times \mathbf{B} + \frac{B}{\omega_c} d_t(\mathbf{v})$$

The rest of the system is identical to the one that was used in the previous studies like Belmont *et al.* [1995], with a scalar pressure and an adiabatic (polytropic) closure assumption. In the frame of the monochromatic linear study that is performed, the additional electric field $\Delta \mathbf{E} = B/\omega_c d_t(\mathbf{v})$ scales like $\alpha = \omega/\omega_c$ with respect to the first term in the Ohm's law: $-\mathbf{v} \times \mathbf{B}$. In addition to the ion inertia term, a term in $\nabla \cdot (\bar{\mathbf{p}})$ should also be introduced to be complete and take into account the effects of finite Larmor radius (function of k_\perp). However, this would be a priori much more complicated since it would imply to calculate the pressure tensor $\bar{\mathbf{p}}$ kinetically.

As long as we assume a pressure scalar and determined by a closure equation $p = p(\rho)$, this term has strictly no effect. In this limit, the system used is fully equivalent to the so-called Hall-MHD system where $\Delta \mathbf{E}$ is usually given in terms of the Hall force $\mathbf{j} \times \mathbf{B}$ (see Appendix A). Accounting for the additional term $\Delta \mathbf{E}$, even when it is small, considerably modifies the resolution of the problem because it changes the differential equation from second to fourth order. The numerical resolution will be presented in section 4.

Another simple case can be considered before solving the general case, it is the cold plasma approximation ($\beta = 0$). In that case, it can be shown that the equation remains a second order one. The solutions are very similar to the solutions obtained in the case $\alpha = 0$ [De Keyser *et al.*, 1999], except that there are two propagation modes instead of three, and therefore there is no case with two resonances.

3. Some Characteristics of the Solutions Deduced From the Homogeneous Dispersion Relation

Let us first consider the general case ($\alpha \neq 0$ and $\beta \neq 0$) when there is no rotation of the magnetic field and discuss the dispersion relation of the linear modes propagating in a homogeneous medium. It is plotted on Figure 2b, and the

dispersion relation for the $\alpha = 0$ case (pure MHD) is plotted on Figure 2a for comparison. This last case is just a particular case of the general one; therefore the same modes appear on the two figures. For one given ω the dispersion relations turn up to be the surfaces in the 3-D \mathbf{k} space where a real propagation is possible. The dispersion equation has a cylindrical symmetry around the direction z of the static magnetic field, so that k_x and k_y have the same role in an homogeneous medium. What is plotted in Figure 2 is the projection of these dispersion surfaces onto the magnetopause plane. The gray shading corresponds to the projection of only one surface, which means that for a given \mathbf{k}_T there is one solution for k_z ; the black shading corresponds to the projection of two surfaces, i.e., two solutions for k_z . The central elliptic region corresponds to the fast mode in both cases a and b. The Alfvén mode corresponds to the lines at $k_z V_A / \omega = \pm 1$ in the MHD case a and to the large region

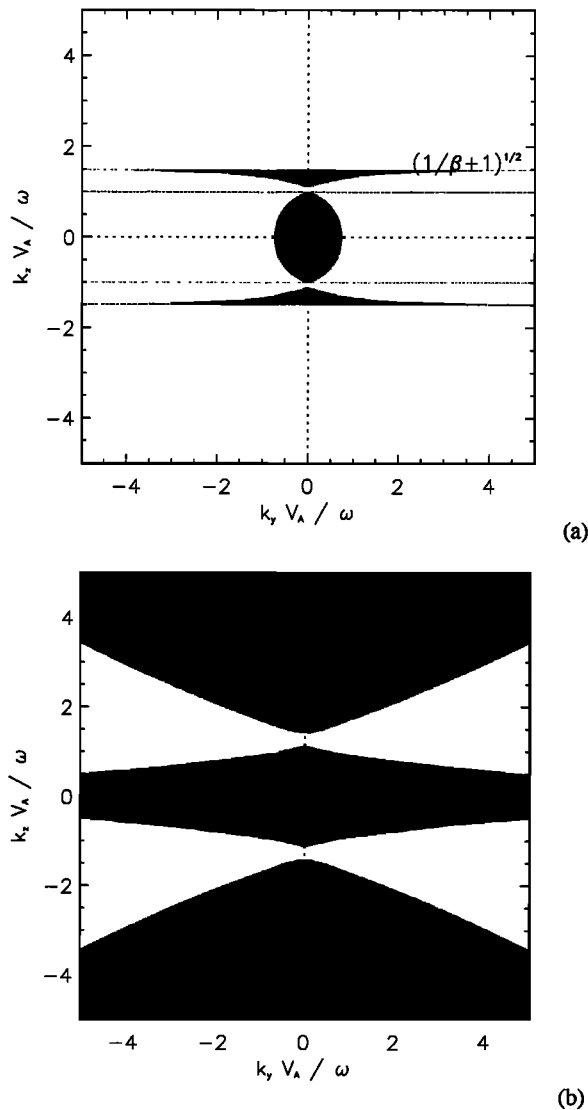


Figure 2. Projection of the dispersion relation in the $(k_y V_A / \omega, k_z V_A / \omega)$ plane for two cases: (a) $\alpha = 0$ and $\beta = 0.8$ and (b) $\alpha = 0.5$ and $\beta = 0.8$. The white regions of the plane correspond to cases where no propagating mode exist (all waves are evanescent), the gray regions correspond to cases where one mode can propagate and the black regions to cases where two modes can propagate.

extending along $k_z V_A / \omega = 0$ in the Hall-MHD case b. The outermost symmetrical regions correspond to the slow mode.

These plots can be used to predict the behavior of the incident wave. When crossing the boundary from the magnetosheath to the magnetosphere, the tangential component of the wave vector is invariant, but the Alfvén velocity increases. Therefore the projection of the wave vector on the $(k_y V_A / \omega, k_z V_A / \omega)$ plane behaves as shown on Figure 3a. As the incident wave is assumed to propagate on the fast mode, the corresponding projection of $\mathbf{k} V_A / \omega$ always lies initially inside the central elliptic region of Figure 2. Afterwards, a conversion to (or a coupling with) the Alfvén mode is possible if, at some points inside the boundary, the $\mathbf{k} V_A / \omega$ vector intersects the corresponding sheet. The situation is very different in both cases: in Figure 2a, this can happen only at one point, in Figure 2b, this can happen for a wide set of points, since in all the central region both the Alfvén and the fast mode can propagate. A resonance can occur in the $\alpha = 0$ case because, in this case, k_x can tend to infinity when approaching the only point in the layer where the Alfvén mode propagates. In the general case, once it has been created, the Alfvén mode can propagate freely back to the magnetosheath and there is no more resonance. This conclusion has been confirmed by the resolution of the differential equation.

The preceding use of the dispersion relation has been presented in the particular case of a magnetic field that does not experience any rotation at the magnetopause. In the more realistic, and more interesting, case of a rotating magnetic field, the method has to be slightly modified. In Figure 2 the direction of the magnetic field was the constant z direction. Considering the rotation of the magnetic field would therefore mean rotating the picture around the x axis direction (perpendicular to the plot). It is similar and simpler to keep the plots such as they are and rather rotate the wave vector, which means that its extremity will not move on a straight line but on a curve, when going from the magnetosheath to the magnetosphere (Figure 3b). It is worth noticing that in many situations, when the rotation angle is sufficient, the wave vector will happen to cross the $k_z = 0$ plane where the Alfvén mode stops propagating. As mentioned earlier, the gray regions in the plane (Figure 2) must be understood as surfaces. This means that the Alfvén mode dispersion region on Figure 2b has to be viewed as a double hat, one on the right side (for $k_z > 0$) and one upside down (for $k_z < 0$). The asymptotic plane $k_z = 0$ therefore separates these two different regions with no possibility of Alfvén propagation between them ($k_1 \rightarrow \infty$). This introduces a mathematical singularity in the resolution of the dispersion equation that we will have to deal with.

4. Resolution Method and Solutions

To transform and solve the Hall-MHD system of equations that has been described in section 2, we use of a mathematical software (Mathematica) allowing both algebraic and numerical computations. We use this software first to eliminate all the unknowns but one, so obtaining a fourth-order differential equation of the last unknown, where the coefficients are algebraic functions of x . The unknown function can be for instance v_y . It is easier to use one only unknown and its first derivatives than the original 11 unknown of the system to define properly the limit conditions. The coefficients, which come from the inversion of a 10×10

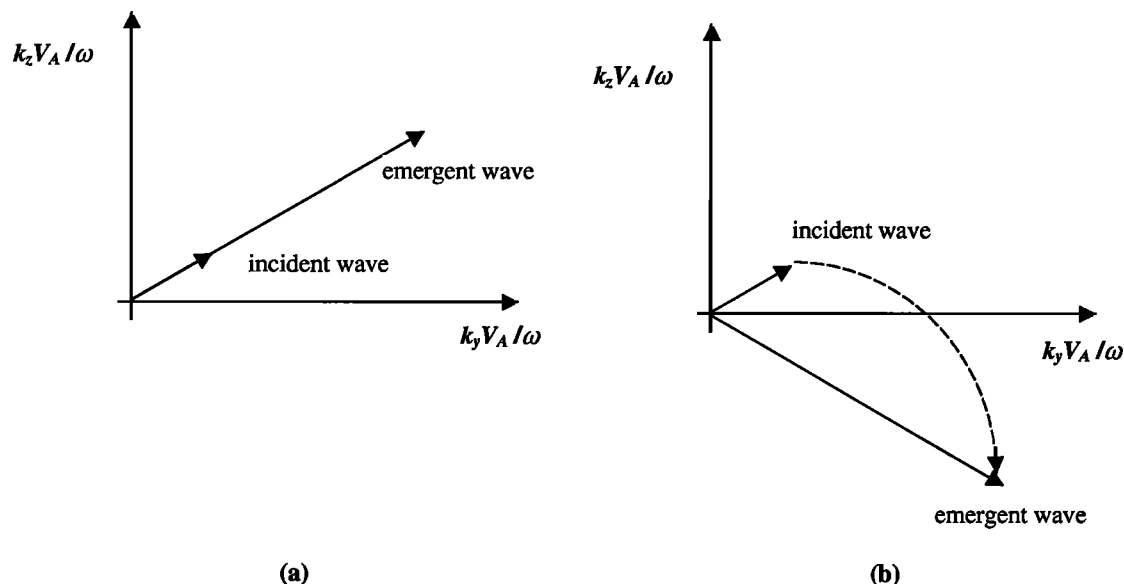


Figure 3. Evolution of the projection of the wave vector in $(k_y V_A / \omega, k_z V_A / \omega)$ plane as the wave crosses the magnetopause layer: (a) without rotation of the magnetic field and (b) with rotation of the magnetic field.

system, have quite huge expressions (each occupying a file of ~ 1 Mbyte) and are then transformed into numerical interpolating functions. As we need a great accuracy for the solutions, the functions are computed with a large number of significant digits. The differential equation is then solved numerically.

In the absence of magnetic field rotation (Figure 4), no singularity occurs and the integration does not need any special caution. It is to be noticed in particular that contrary to the results obtained in ideal MHD [Belmont *et al.*, 1995, De Keyser *et al.*, 1999], there does not exist any trace of the resonant amplification mechanism. The technique to find out a solution respecting the limit conditions, both on the left and on the right side, is described in Appendix B. This technique is composed of three main steps: (1) find the general form of the solutions respecting the left side limit conditions (three free parameters), (2) idem on the right side (two free parameters); (3) ensure the continuity of the final solution in the calculation domain (four equations). This entire program has been performed to obtain Figure 4. The physical interpretation, in terms of the homogeneous wave modes, is sketched in Figure 5. It is worth noticing that even in this simple case without singularity, the method can be quite difficult to handle numerically. As the Alfvén mode is characterized by very short scales in the x direction, it can decrease by a huge factor between $x = 0$ and the right end of the computation domain in the most general case when it is evanescent in the magnetosphere. In these conditions, integrating back, as we have to do, from the right end to $x = 0$ tends to be an ill-posed problem and demands a very great numerical accuracy (we worked generally with an accuracy of 50 significant digit).

When the magnetic field rotation is taken into account, the most interesting situation occurs when a point where $k_{\parallel} = 0$ exists in the layer. A typical result obtained in this case is presented in Figure 6, and it will be analyzed from a physical point of view in the next section. Technically, the singularity brought by the point $k_{\parallel} = 0$ is much more difficult to overcome than the usual logarithmic singularity occurring in

ideal MHD due to the Alfvén resonance (in this case, the addition of an imaginary part to the tangential wave vector was sufficient). In the vicinity of this point, two solutions (on the magnetosonic mode) are regular and two (on the Alfvén mode) are singular, with a wavelength tending to zero and an amplitude which also decreases to zero. For solving, it is then quite mandatory to split the integration domain into two parts around the position $x = x_s$, where the singularity occurs. The same procedure as previously can then be applied, except that the equations of continuity to be written to determine the four coefficients are more difficult (see Appendix B).

All these operations are long and require skilful handling. These difficulties of course amplify the questions of numerical accuracy already emphasized for the case without magnetic field rotation. It is, nevertheless, the best way we found to treat this problem. It is to be expected that future workers in this field will find simpler and more robust mathematical methods.

5. Absence of Alfvén Resonance

One of the most striking features of the preceding results is the absence of Alfvén resonance. It seems therefore that the phenomenon of resonant amplification, evidenced by Belmont *et al.* [1995], was an artifact of the ideal MHD model. A priori, this conclusion also holds for all the studies that have been published for almost thirty years concerning resonant absorption in a magnetized plasma, as well in the space physics context as in fusion studies and solar physics [e.g., Southwood, 1974; Chen and Hasegawa, 1974a, 1974b; Zhu and Kivelson, 1988, 1989; Grossman and Smith, 1988]. As soon as a nonideal term is added in the Ohm's law (in this paper, the ion inertia term), this phenomenon completely disappears. There is no continuity, in the given geometry, between the pure MHD solution (with a divergence) and the nonideal MHD solution (with no divergence and even no remnant peak), whatever the smallness of the nonideal effect added. This surprising result had never been properly

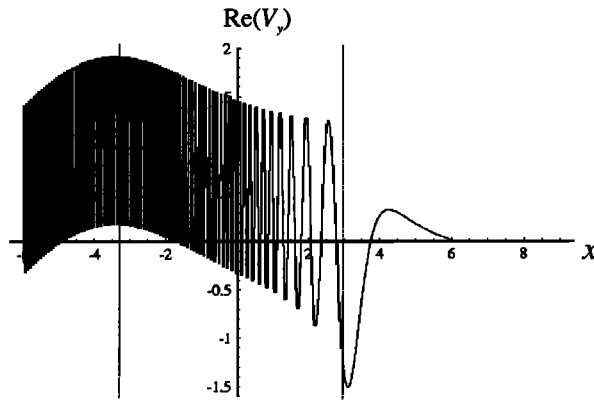


Figure 4. Solution without rotation. The quantity plotted is the real part of the v_y component of the velocity (y is the tangential direction perpendicular to \mathbf{B}). The two dashed lines crudely indicate the limits of the magnetopause gradient (thickness of ~ 600 km).

evidenced and analyzed hitherto, although it is reminiscent of the claim by *Bellan* [1994] that Alfvén resonance does not exist at all, even in cold plasma. Our result, which obviously does not invalidate all ideal MHD results, is different: it only outlines a misbehavior of this theory for propagation in a *strictly* perpendicular gradient, this misbehavior disappearing when ion inertia effects or finite Larmor radius effects are introduced simultaneously with a finite temperature.

The interpretation of this effect is not self evident but can be found from considerations about the order of the differential equations, and with the help of the homogeneous dispersion equation presented in section 3. In the MHD range, three modes of propagation exist, which means that the dispersion equation should a priori be of order 6 with respect to any component k_i of the wave vector. If a gradient is present in the background in one given direction \mathbf{e}_n , any plane wave keeps constant the tangential component \mathbf{k}_T of its wave vector, and the propagation in direction \mathbf{e}_n is therefore determined in general by six limit conditions. This conclusion

is physically correct, and it is in general well respected by any model, ideal MHD, Hall-MHD, or others.

Nevertheless, there is one case where ideal MHD does not respect this conclusion, that is the case when the gradient is strictly perpendicular to the static magnetic field. Because of its own approximation, ideal MHD then provides a dispersion equation which is only quadratic with respect to the perpendicular component of the wave vector k_\perp (but remaining sixth order in k_\parallel). The propagation in any perpendicular direction x is therefore determined by a differential equation that is of second order only and two limit conditions are sufficient to determine it. It means that the only possible exchanges in the inhomogeneous medium are then those existing at each point of the layer between the incident wave and the reflected one, both waves belonging to the same mode (and differing only by their opposite propagation directions). When going across the layer, this unique mode is successively a fast, an Alfvén and a slow mode. At the only point of the layer for instance where the mode is a propagating Alfvén mode (*i.e.* where $\omega = k_\parallel V_A$), the energy propagation becomes strictly parallel and the perpendicular energy flux approaching this point cannot be evacuated any more. It is the essential reason of the amplitude divergence. A similar argument holds for the asymptotic plane of the slow mode, which also gives rise to a divergence.

It is worth noticing that even in ideal MHD, this behavior is singular with respect to the direction of the gradient. It disappears as soon as the gradient is not strictly perpendicular to the static magnetic field (*i.e.*, a layer different from that of a tangential discontinuity), even for an infinitely small departure from the perpendicular direction. This misbehavior of ideal MHD with respect to perpendicular propagation is cancelled when any nonideal effect is added to the MHD system. In Hall-MHD for instance, the coupling between Alfvén and compressional modes makes the perpendicular propagation come to a fourth order so that all modes become propagating, and no divergence occurs. In this case, as in the general one, Alfvén and magnetosonic modes exist simultaneously and the inhomogeneity only induces energy transfers from one to the other.

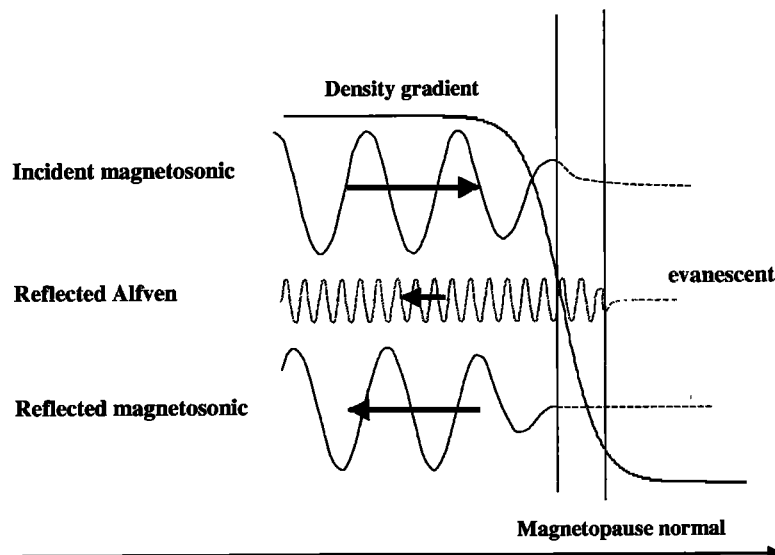


Figure 5. Schematic interpretation of Figure 4.

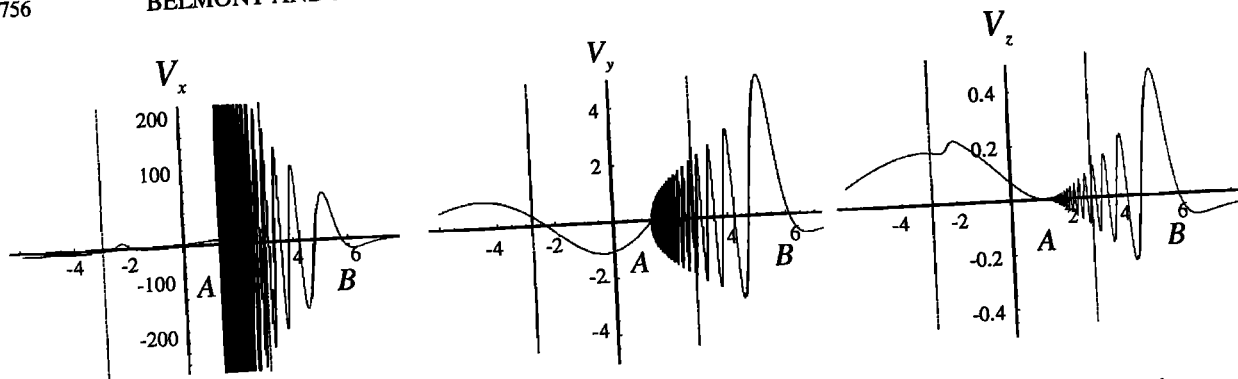


Figure 6. Solution with rotation. The three components of the velocity are plotted in a rotating frame (y and z rotate with the magnetic field). A and B refer to the points where (a) $k_{||} = 0$ and where (b) the Alfvén mode becomes evanescent.

6. Trapping of an Alfvén Wave in the Boundary

In Figure 6, as in Figure 4, the parameters correspond to a plasma parameter $\beta = 0.1$ and a coefficient $\alpha = \omega/\omega_d$ of 0.05. These parameters have not been chosen to represent realistically the magnetopause where β is of the order of unity. They have been chosen to outline how much the results are different from those obtained with $\alpha = \beta = 0$ as in the work of Belmont *et al.* [1995] even when the departures from these conditions are small. This drastic difference appears as soon as α and β simultaneously are chosen different from zero. If one only of these coefficients remains null (see, for instance, De Keyser *et al.* [1999], for the case $\alpha = 0$), the differential equation remains of second order and the resonances occur (see the appendix and the discussion below). The difference between Figures 6 and 4 comes from the presence of a point $k_{||} = 0$, in Figure 6, thanks to the magnetic field rotation. The interpretation of what happens is sketched in Figure 7. On the left side of the singularity, a small incident magnetosonic wave impinges the magnetopause. In the magnetopause gradient a large part of this incident energy is converted in a reflected magnetosonic wave, giving rise to a standing wave, and a negligible part goes to the Alfvén mode.

On the right side the coupling toward the Alfvén mode becomes more and more efficient as x approaches the point where $\omega = k_{||}V_A$. The part converted into a forward Alfvén wave is rapidly vanishing (point B of Figure 6), but the backward Alfvén wave comes back toward the magnetosheath and stops propagating at the singularity (point A of Figure 6). In this way, a strong Alfvén wave is trapped inside the boundary. This result is important for two reasons: (1) It gives a new and realistic interpretation to the strong amplitude of the fluctuations that are observed at the magnetopause (and it should lead to a quantitative estimate of this amplification while the theory of resonant amplification did not allow it). (2) The large level of a Hall-MHD Alfvén wave in the layer could provide an explanation to the magnetic flux and plasma transfer through the magnetopause (see next section).

7. Microreconnection

As long as the magnetopause is described at any time and any place in an ideal MHD frame, any leak, of magnetic flux or of matter, is forbidden through the boundary. We will try now to estimate to what extent the adopted Hall-MHD

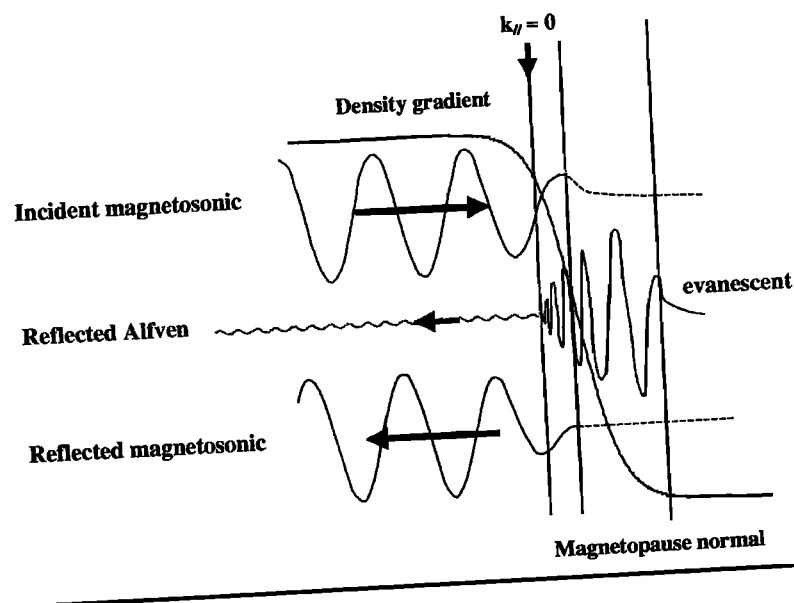


Figure 7. Schematic interpretation of Figure 6.

formalism, by taking into account a finite $\omega = \omega/\omega_{ci}$ ratio (appendix A), allows to explain the observed penetrations from the solar wind into the magnetosphere. It can be observed that the role of the Hall effect for spontaneous (unstable) reconnection has focused an increasing interest for a few years (e.g., *Battachejee et al.* [1999] or *Shay et al.* [2001]). Our goal is nevertheless different since we want to estimate, for a stable magnetopause, the reconnection rate related to magnetic fluctuations that preexist in the magnetosheath and propagate across the boundary.

In a general way, let us characterize the departure from ideal MHD by an additional electric field $\Delta\mathbf{E}$ appearing in the Ohm's law:

$$\mathbf{E} = -\mathbf{v} \times \mathbf{B} + \Delta\mathbf{E}$$

With this notation the temporal variation of the magnetic field, in the frame moving with the plasma flow, can be determined via some handling of the Maxwell equations:

$$d_t(\mathbf{B}) = \mathbf{B} \cdot \overline{\mathbf{M}} - \nabla \times (\Delta\mathbf{E})$$

where $\overline{\mathbf{M}}$ is a tensor defined as:

$$\overline{\mathbf{M}} = \nabla(\mathbf{v}) - \nabla \cdot (\mathbf{v}) \overline{\mathbf{I}}$$

In order to estimate the magnetic flux leakage through an elementary surface $\delta\mathbf{S}$, it is also necessary to determine the temporal variation of the surface, when carried along by the flow. Some new algebra leads to:

$$d_t(\delta\mathbf{S}) = -\overline{\mathbf{M}} \cdot \delta\mathbf{S}$$

Considering the magnetic flux $\delta\Phi = \mathbf{B} \cdot \delta\mathbf{S}$ across an elementary surface $\delta\mathbf{S}$, its variation immediately follows:

$$d_t(\delta\Phi) = -[\nabla \times (\Delta\mathbf{E})] \cdot \delta\mathbf{S}$$

Let us first notice that, in the case of an ideal Ohm's law, i.e., when $\Delta\mathbf{E} = 0$, this expression results in well-known consequences. It first entails $\delta\Phi$ remaining constant when \mathbf{B} and $\delta\mathbf{S}$ are carried along the flow, from which two classical results of ideal MHD can be derived: (1) Taking a vector $\delta\mathbf{S}$ aligned with \mathbf{B} , the magnetic flux $\delta\Phi_{\parallel}$ in a flux tube is conserved along the flow; (2) Taking a vector $\delta\mathbf{S}$ initially perpendicular to \mathbf{B} , the flux $\delta\Phi_{\perp}$ remains zero along the flow, i.e., no magnetic leakage is allowed perpendicularly to the flux tube (i.e., no reconnection).

In the presence of a nonzero $\Delta\mathbf{E}$, the preceding formula, for $\delta\mathbf{S}$ perpendicular to \mathbf{B} , provides an expression for the rate of magnetic flux reconnected per second across the surface $\delta\mathbf{S}$. For characterizing this reconnection rate in any direction, let us finally define the vector:

$$\boldsymbol{\tau} = -\frac{\nabla \times (\Delta\mathbf{E})}{B} \cdot \overline{\mathbf{D}}_{\perp}$$

where $\overline{\mathbf{D}}_{\perp} = \overline{\mathbf{I}} - \mathbf{e}_{\parallel} \mathbf{e}_{\parallel}$ is the projector onto the plane perpendicular to \mathbf{B} (noting $\mathbf{e}_{\parallel} = \mathbf{B}/B$ the unit vector in the direction of \mathbf{B}). Each component τ_{α} of $\boldsymbol{\tau}$ therefore represents the flux reconnected per second through any surface $\delta\mathbf{S} = \delta S \mathbf{e}_{\alpha}$, divided by the flux $B\delta S$ in a flux tube of section δS . In other words, one can calculate the flux reconnected through any perpendicular surface $\delta\mathbf{S}$ by:

$$d_t(\delta\Phi_R) = B \boldsymbol{\tau} \cdot \delta\mathbf{S}$$

Concerning the linear model presented in section 2, $\boldsymbol{\tau}$ can be expanded with respect to the small parameter

characterizing the wave amplitude (order 1). The zero order (equilibrium) rate τ_0 is null since the zero order is supposed stationary (and therefore $\Delta\mathbf{E}_0 = 0$); the first order τ_1 is non zero, but its time-averaged value remains zero for a monochromatic wave. So, the first interesting term to estimate is the time-averaged value of the second order term $\langle \tau_2 \rangle$:

$$\langle \tau_2 \rangle = -\left[\nabla \times \left(\frac{\langle \Delta\mathbf{E}_2 \rangle}{B_0} \right) \right] \cdot \overline{\mathbf{D}}_{\perp 0} - \left[\nabla \times \left(\frac{\Delta\mathbf{E}_1}{B_0} \right) \right] \cdot \overline{\mathbf{D}}_{\perp 1}$$

We will further specify the $\Delta\mathbf{E}$ involved is the ion inertia term (equivalent to the Hall-MHD term, see appendix A):

$$\Delta\mathbf{E} = \frac{B}{\omega_c} d_t(\mathbf{v})$$

and that we look for the reconnection rate $\langle \tau_{2x} \rangle$ in the x direction normal to the equilibrium magnetopause. In these conditions, the first term is exactly zero because it only involves derivatives with respect to y and z while the mean value $\langle \Delta\mathbf{E}_2 \rangle$ only depends on x . The second one leads to:

$$\langle \tau_{2x} \rangle = \frac{\omega}{2\omega_{co}} \text{Im} \left\{ \frac{B_{1x}}{B_0} [\nabla \times (\mathbf{v}_1^*)] \cdot \mathbf{e}_{\parallel 0} \right\}$$

where the star indicates a complex conjugation. It is worth noticing that the rate of reconnected flux is proportional to ω/ω_{co} , pointing out the necessity of the Hall-MHD description. From a quick analysis of this result, one can see that it depends on the fluctuation level through a combination of B_1 and \mathbf{v}_1 components that is crudely proportional to $|\mathbf{v}_{1x}^2|$.

The reconnection rate is therefore determined by the upstream fluctuation spectrum in the magnetosheath, increased in the boundary, for each frequency ω , by a factor proportional to k_x^2 if the x energy flux is conserved (k_x^{-1} being the local x scale). The result is therefore maximum for the minimum scale reached, which is likely to be determined by the Larmor radius. When this effect is neglected, the reconnection rate is found to tend to infinity when approaching the critical point. On the contrary, accounting for this effect would give the dependence of the result on the ratio between the Larmor radius and the magnetopause thickness.

When applied to the numerical results of our model, the above expression provides the time-averaged reconnection rate plotted on Figure 8. The main point to be noticed is that the reconnected flux is well localized in the layer and that it is always strictly positive, i.e., directed from the magnetosheath toward the magnetosphere. The time-averaged magnetic flux leakage from a plasma tube is therefore always in the earthward direction, as expectable. This result is physically satisfactory: when they reach points where the reconnection rate is noticeable, the magnetic flux tubes stop sticking tightly to the plasma tubes and, thanks to ion inertia, they can separate and disalign from them. Afterward, as soon as they reach a point where the reconnection rate goes back to zero, they start again to align with a new plasma tube and to travel together with it. From a particle point of view, the disalignment between flux and plasma tubes allows to get "reconnected" field lines along which particles are free to penetrate the magnetosphere. The modulation observed on Figure 8 in the magnetic reconnection rate corresponds to the interferences existing between the short scale Alfvén mode and the large-scale magnetosonic mode. The second point to

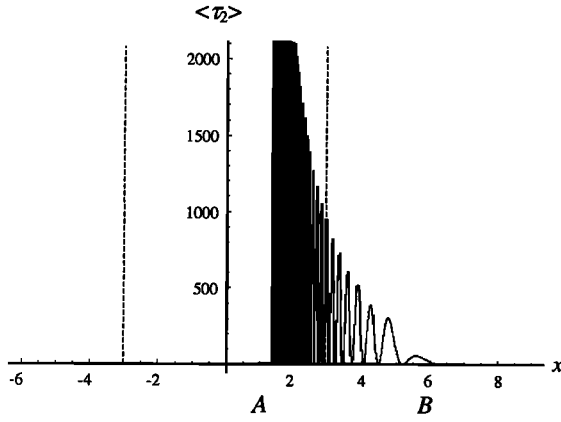


Figure 8. Reconnection rate in the x (normal) direction, calculated for the solution with rotation (Figure 6). The result evidences the localization of the reconnection phenomenon, but the numerical values (in ω_{ci} unit) can be disregarded.

be noticed is that the numerical values obtained appear fully unrealistic: the reconnection rate goes to infinity at the critical point x_c and is still of thousands of ω_{ci} at ~ 100 km apart from it. This much too fast reconnection is clearly related to the fact that the finite Larmor radius effects are not taken into account while, with the numerical values used, wavelengths in the layer occur to be much less than the Larmor radius. A quantitative comparison with experiment or with preceding models (as the model of stochastic transport by *Rosenbluth et al.* [1966]) cannot therefore trustingly be undertaken before finite Larmor radius are included in the model.

8. Discussion and Conclusion

This paper belongs to a series of studies initiated by *Belmont et al.* [1995] and investigating the origin and the role of the strong magnetic turbulence observed at the magnetopause. Two main new ingredients have been added with respect to the preceding studies: the ion inertia is taken into account in the Ohm's law (equivalent to Hall-MHD model, see Appendix A) and the magnetic field rotation at the magnetopause allows for a point where $k_{||} = 0$. The first point allows to get Alfvén waves that can propagate in the normal x direction. The second introduces a point where this propagation stops.

Three important conclusions have been drawn:

1. The phenomenon of resonant amplification, evidenced by *Belmont et al.* [1995], appears as an artifact of the ideal MHD model. This conclusion a priori also holds for all Alfvén resonance absorption phenomena as studied for almost 30 years. Resonant absorption appears as a misbehavior of ideal MHD for propagation in a strictly perpendicular gradient, this misbehavior disappearing when ion inertia effects (or finite Larmor radius effects) are introduced simultaneously with a finite temperature.

2. A major role is played by the magnetic rotation. For all incident waves crossing a point where $k_{||} = 0$, there is a possibility of trapping a strong Alfvén wave inside the layer. This Alfvén wave is very likely to be the cause of the amplification of the fluctuations observed at the magnetopause. Furthermore, it is also likely to be the cause of the penetration of magnetic flux into the magnetosphere.

3. Thanks to the trapped Alfvén wave, a noticeable rate of reconnection can be provided. The magnetic flux penetrating

the magnetosphere is therefore directly monitored, in the present model, by the magnetosheath turbulence. This scenario can be at the origin of a drastic change of paradigm concerning the transfers through the magnetopause. In classical stationary reconnection, an exterior electrostatic field is assumed and determines the reconnection rate. In nonstationary reconnection models an inductive self consistent electric field is assumed to play the same role, but the nonstationarity and the subsequent field are always supposed to be related to the development of an instability (in general a tearing instability). As, in many circumstances, it can be demonstrated that the layer is not unstable, it is often hastily concluded that no reconnection occurs. As a matter of fact, the absence of reconnection is a consequence of ideal MHD and we have shown that the small scales related to the turbulence are sufficient to break the validity of this assumption. A way of estimating the reconnection rate in this context has been provided. It is worth noticing that the phenomenon invoked can be distributed everywhere on the magnetopause surface, contrary to the classical models of reconnection, which are localized at some X points, but similarly to the model of "patchy reconnection" of *Galeev et al.* [1986]. However, this last model grounds, as the preceding ones, on some ("microtearing") instabilities.

The validity of the results presented in this paper is a priori limited by the fact that the model does not correctly describe the wavelengths smaller than the gyroradius. This problem remains to be investigated, but we can guess that the finite Larmor radius effects will rather be a limitation than a cause for reconnection. In our model, the wavelength of the Alfvén mode tends toward zero near $k_{||} = 0$ and the reconnection rate due to the Hall effect tends to infinity. The finite Larmor effects will certainly limit the minimum wavelength and taking them into account should therefore allow for a more realistic estimate of the reconnection rate.

Appendix A: Ion Inertia and Hall-MHD Model

For frequencies much smaller than the electron plasma frequency, quasi-neutrality is verified and the momentum equations, for ions and electrons can be written:

$$\begin{aligned} nm_i d_t(\mathbf{v}_i) &= ne(\mathbf{E} + \mathbf{v}_i \times \mathbf{B}) - \nabla(p_i) \\ nm_e d_t(\mathbf{v}_e) &= -ne(\mathbf{E} + \mathbf{v}_e \times \mathbf{B}) - \nabla(p_e) \end{aligned}$$

In monofluid theories these two equations are replaced by two different ones. The first one is the sum:

$$nmd_t(\mathbf{v}) = \mathbf{j} \times \mathbf{B} - \nabla(p) \quad (1)$$

where $p = p_i + p_e$ is the total pressure; m and \mathbf{v} are characteristics of the global fluid: $m = m_i + m_e \approx m_i$, and $\mathbf{v} = m_i / m \mathbf{v}_i + m_e / m \mathbf{v}_e \approx \mathbf{v}_i$.

The second equation is a generalized Ohm's law and it can be found under different forms depending on the authors. Neglecting the electron mass (i.e., identifying \mathbf{v} with \mathbf{v}_i and m with m_i), the simplest way to derive this equation is just to keep unchanged the ion momentum itself:

$$\mathbf{E} = -\mathbf{v} \times \mathbf{B} + \frac{m}{e} d_t(\mathbf{v}) + \frac{1}{ne} \nabla(p_i) \quad (2)$$

In collisional plasmas, a fourth term \mathbf{j}/σ should be added, σ being the resistivity. This well known term (the unique one in the classical Ohm's law in a metallic conductor) has not to be introduced here since the magnetopause medium can be considered as strictly collisionless with a great accuracy.

In this paper, we use a simplified version of equation (2) by only retaining the ion inertia term:

$$\mathbf{E} = -\mathbf{v} \times \mathbf{B} + \frac{m}{e} d_i(\mathbf{v}) \quad (3)$$

The reason for disregarding the last term is that the rotational of $(1/ne)\nabla(p_i)$ is identically zero in the hypotheses considered. As a matter of fact, $\nabla \times [\nabla(p_i)]$ is zero as long as the pressure is assumed scalar, and $\nabla(n) \times \nabla(p_i)$ is zero as long as a closure equation $p_i = p_i(n)$ is assumed (these terms would lead to finite Larmor radius effects in other hypotheses and would then intervene for short wavelengths). As the system solved only depends on the inductive electric field (components corresponding to a rotational $\nabla \times (\mathbf{E}) \neq 0$), and as it is strictly independent on the electrostatic part of the electric field (deriving from a gradient), this argument shows that the pressure term, in our hypotheses, would not lead to any change in the results (except the electric field itself).

The generalized Ohm's law used classically in the Hall-MHD system is different from (2) but can be derived easily from it. In this original equation, if one eliminates the ion inertia term with the help of (1), it becomes

$$\mathbf{E} = -\mathbf{v} \times \mathbf{B} + \frac{1}{ne} [\mathbf{j} \times \mathbf{B} - \nabla(p_e)] \quad (4)$$

This is the classical Hall-MHD form of Ohm's law. However, for the same reasons as above, the last term, containing the electron pressure, can be ignored because it leads to zero inductive electric field. It is therefore sufficient to retain the term evidencing the Hall effect:

$$\mathbf{E} = -\mathbf{v} \times \mathbf{B} + \frac{1}{ne} \mathbf{j} \times \mathbf{B} \quad (5)$$

One can therefore use indiscriminately one or the other form (3) or (5) which are strictly equivalent: in the hypotheses considered, both terms $(m/e)d_i(\mathbf{v})$ or $(1/ne)\mathbf{j} \times \mathbf{B}$ contribute to the same inductive electric field as it can be seen directly on (1). These terms therefore intervene for finite frequencies, at the difference from the finite Larmor radius effects, which intervene for small wavelengths.

Appendix B. Numerical Solutions Techniques

A1. Without Magnetic Field Rotation

The magnetopause gradient is confined in x to a limited layer (Figure 1); therefore the solution $s(x)$ must tend, for large $|x|$ on both sides, toward a combination of the homogeneous medium solutions (HMS) $h_i(x)$, which are known analytically. As we consider the problem of one only incident magnetosonic wave coming from the left side (magnetosheath), we have to impose that the solution tends, for $x < 0$, to a combination of three HMS: one forward h_1 (magnetosonic) and two backward h_2 and h_3 (magnetosonic and Alfvén). For $x > 0$, as no wave comes from the right side, the solution must tend to a combination of two forward HMS h_4 and h_5 (magnetosonic and Alfvén).

The numerical integration of the differential equation is first performed five times, three times from the left and twice from the right. We calculate in this way the five partial solutions that coincide with the five HMS asymptotically: (s_1, s_2, s_3) coinciding with (h_1, h_2, h_3) for $x \rightarrow -\infty$, and (s_4, s_5) coinciding with (h_4, h_5) for $x \rightarrow +\infty$. One must therefore be able to write the solution $s(x)$ both as a combination of the three left solutions $s = a_1 s_1 + a_2 s_2 + a_3 s_3$, and as a combination

of the two right solutions $s = a_4 s_4 + a_5 s_5$, the five coefficients remaining to be determined. Knowing that these two forms of the solution must be identical at any point of the integration domain, we can for instance choose to write this identity (for $s(x)$ and its three first derivatives) in $x = 0$. This provides four equations, which allow the determination of the four coefficients (a_2, a_3, a_4, a_5) . The first coefficient a_1 is the amplitude of the incident wave and remains arbitrary in our linear problem (we take it equal to 1).

A2. With Magnetic Field Rotation

The first steps are identical as above. Five particular solutions s_i are again determined, three respecting the boundary conditions on the left side and two on the right side. Each of these solutions are determined up to the critical point x_c where the equation is singular. The most difficult part then consists in writing the correct "continuity" equations through x_c . We proceed as follows:

1. A basis of four local solutions b_i is determined analytically in the vicinity of the singularity by expanding the differential equation around this point. One finds two regular solutions varying locally as $\exp[ik_\perp(x-x_c)]$, and two singular solutions varying as $|x-x_c|^{p_\pm}$. The two values k_\pm are determined from the coefficients of the differential equation by a quadratic equation. The two values p_\pm are complex conjugate and are determined similarly (their common real part is negative, and the imaginary part is positive for p_+ and negative for p_-). The absolute value, in the form of the singular solutions, is necessary in order to get the same determination on both sides of the singularity for each solution. It corresponds to a causal continuity between the incident part of the solution and its continuation on the opposite side. Nevertheless, it has to be noticed that this choice introduces an enormous ratio $\exp[p_+/\pi]$ between the amplitudes on both sides (with $p_+ = \text{Im}(p) \approx 55$), which means that there is a quasi-null transmission of information on the Alfvén mode through the point $k_\parallel = 0$. This result is not physically surprising since the Alfvén mode, as deduced from the homogeneous dispersion equation, stops propagating at this point.

2. At two points very close to the singular point $x_s \pm \varepsilon$, each of the five solution s_i is decomposed on the four preceding analytical modes b_i ; this is done by using the value of this solution and of its three first derivatives.

The coefficients of the linear combination can then be calculated. The four continuity equations providing these coefficients are no more those of the solution and its three first derivatives as previously. Instead, we now have to write that the decomposition of the solution on the local basis is identical on both sides of the singularity.

Acknowledgments. We are pleased to acknowledge Fabien Reberac's work: he has been the first to evidence the mathematical difficulties related with the use of Hall-MHD for the search of resonances. This paper results from numerous discussions with him to understand the origin of these difficulties.

Michel Blanc thanks Lev Zelenyi and another referee for their assistance in evaluating this paper

References

- Bhattacharjee, A., Z.W. Ma, and X. Wang, Impulsive reconnection dynamics in collisionless laboratory and space plasmas, *J. Geophys. Res.*, **104**, 14,543-14,556, 1999.
- Bellan, P.M., Alfvén resonance reconsidered: Exact solutions for wave propagation across a cold inhomogeneous plasma, *Phys. Plasmas*, **1**(11), 3523-3541, 1994.

- Belmont, G. and L. Rezeau, Finite Larmor radius effects : The two-fluid approach, *Ann. Geophys.*, **5A**, 59-70, 1987.
- Belmont, G., F. Reberac, and L. Rezeau, Resonant amplification of magnetosheath MHD fluctuations at the magnetopause, *Geophys. Res. Lett.*, **22**, 295-298, 1995.
- Berchem, J., and C. T. Russell, Magnetic field rotation through the magnetopause: ISEE 1 and 2 Observations, *J. Geophys. Res.*, **87**, 8139-8148, 1982.
- Chen, L., and A. Hasegawa, A theory of long-priod magnetic pulsations, Steady state excitation of field line resonance, *J. Geophys. Res.*, **79**, 1024-1032, 1974a.
- Chen, L., and A. Hasegawa, Plasma heating by spatial resonances of Alfven wave, *Phys. Fluids*, **17**, 1399, 1974b.
- De Keyser, J., M. Roth, F. Reberac, L. Rezeau, and G. Belmont, Resonant amplification of MHD waves in realistic subsolar magnetopause configurations, *J. Geophys. Res.*, **104**, 2399, 1999.
- Galeev, A. A., M. M. Kuznetsova, and L. M. Zeleny, Magnetopause stability threshold for patchy reconnection, *Space Sci. Rev.*, **44**, 1-41, 1986.
- Grossman, W., and R. Smith, Heating of solar coronal loops by resonant absorption of Alfven waves, *Astrophys. J.*, **332**, 476, 1988.
- Johnson, J. R. and C. Z. Cheng, Kinetic Alfven waves and plasma transport at the magnetopause, *Geophys. Res. Lett.*, **24**, 1423-1426, 1997.
- Rezeau, L., and G. Belmont, Magnetic turbulence at the magnetopause, a key problem for understanding the solar wind/magnetosphere exchanges, *Space Sci. Rev.*, **95**, 427-441, 2001.
- Rezeau, L., A. Morane, S. Perraut, A. Roux, and R. Schmidt, Characterization of Alfvenic fluctuations in the magnetopause boundary layer, *J. Geophys. Res.*, **94**, 101-110, 1989.
- Rosenbluth, M. N., R. Z. Sagdeev, J. B. Taylor, and G. M. Zaslavski, The destruction of magnetic surfaces, *Nucl. Fusion*, **6**, 297, 1966.
- Shay, M. A., J. F. Drake, B. N. Rogers, and R. E. Denton, Alfvenic collisionless magnetic reconnection and the Hall term, *J. Geophys. Res.*, in press, 2000.
- Southwood, D. J., Some features of field line resonances in the magnetosphere, *Planet. Space Sci.*, **22**, 483-491, 1974.
- Zhu, X., and M. G. Kivelson, Analytic formulation and quantitative solutions of the coupled ULF wave problem, *J. Geophys. Res.*, **93**, 8602-8612, 1988.
- Zhu, X., and M. G. Kivelson, Global mode ULF pulsations in a magnetosphere with a non monotonic Alfven velocity profile, *J. Geophys. Res.*, **94**, 1479-1485, 1989.

G. Belmont, and L. Rezeau, CETP/UVSQ, 10-12 Avenue de l'Europe, 78140, Vélizy, France (gerard.belmont@cetp.ipsl.fr, laurence.rezeau@cetp.ipsl.fr).

(Received August 1, 2000 ; revised October 16, 2000 ; accepted October 16, 2000.)